Penerbit Akademia Baru

CFD Letters

Journal homepage: www.akademiabaru.com/cfdl.html
ISSN: 2180-1363

Research On Pentamaran By Model Test And Theoretical Approach Based On Michell's Integral

Open Access

Wiwin Sulistyawati[1], Yanuar[1,*], Agus Sunjarianto Pamitran[1]

[1] Department of Mechanical Engineering, Universitas Indonesia, Depok 16424, Indonesia

ARTICLE INFO

Article history:
Received 3 December 2018
Received in revised form 13 March 2019
Accepted 20 March 2019
Available online 23 March 2019

ABSTRACT

The interaction between hulls, their position and shape and the length of the side hulls of a multihull affect the amount of wave resistance. This paper presents computation based on Michell's theory on the various configurations of pentamaran and correlates with towing test data that involves interference flow around the component hulls. The pentamaran hull form was featuring a warped chine for the main hull recommended by Savitsky and V model for outriggers. Analysis of both transversal and divergent waves was performed to assess the magnitude of wave resistance that occurs due to the placement of the side hull to the main hull. Furthermore, investigations on far-field wave pattern, wave interference, wave resistance as well as total resistance have been conducted. Changing of the side hull on clearance strongly affects the resistance characteristics than stagger. Configuring the pentamaran so that the main hull is placed at the centreline of each of the front-side hull approximately 15°-18°could be an effective manner to reduce resistance. In general, all of the resistance components results showed that Michell's theory agree with the test, particularly at Fn greater than 0.5, in which possible viscous factors were still influential at low speed where the theoretical prediction could not be potentially valuable.

Keywords:
pentamaran; resistance; interference; far field wave pattern; Michell's theory

1. Introduction

In general, there are two types of ship resistance: frictional resistance and wave resistance. Identifying the wave resistance of multihull is very complicated due to the strong influence of things mentioned earlier. Configuration of the multihull in the placement of individual hulls is an attempt to minimise the wave resistance, which also reduces the total resistance. Certainly, it is related to the power energy required to propel the ship, which results in fuel consumption. Ikeda *et al.,* [1] noted that the total resistance of a multihull could be minimised by the shape of the hull and proper configuration of outriggers. According to Oller *et al.,* [2], longitudinal and transverse configurations between hulls are needed so they can be at an optimum placement as they can affect frictional resistance, stability and seakeeping performance.

* *Corresponding author.*
E-mail address: yanuar@eng.ui.ac.id (Yanuar)

Multi-hulls planning has been carried out for several decades. Savitsky and Dingee [3] began by testing parallel flat plate planning at very high Froude numbers. We can also find this test in Ocon *et al.,* [4] for parallel plates in turbulent flow. Research on warp-chine on a multihull by Liu and Wang [5] by a tested series on planning catamaran and suggested an improvement empirical method of a single-hull lift by Savitsky [6]. According to Chengyi [7], symmetrical chine hull on catamarans had minimised the resistance of the waves, with its interference tending to fall to Fn > 0.5. Ackers *et al.,* [8] showed that using symmetrical chine hull had a significant effect on the interference resistance caused by the interaction between the waves and the bow, the main hull and the side hulls. On the contrary, E. O. Tuck and L. Lazauskas [9] showed that symmetrical chine hull gives the lowest resistance and the highest propulsive efficiency. Moraes [10] used symmetrical chine hull at catamaran ships and obtained similar results and compared them with Wigley. Furthermore, Blount [11] showed that chine forms have better dynamic stability at high speeds. The experiment of Begovic and Bertorello [12] showed that ships with a chine hull form have a deadrise angle of 25°, which is better for storm conditions; however, the experiments were conducted under calm water conditions. Furthermore, Bari and Matveev [13] obtained catamaran with chine form on deadrise angle until 20° lift coefficient force increased in line with the increase of deadrise and Fn and with a short distance of outriggers.

Researches on multihull particularly on pentamaran were more dominated by configuration effects of stagger (S_T) and clearance (C_L) with commonly used models such as series NPL, series 60, series 62 and Wigley. Particularly the shape of Wigley was very dominant in pentamaran experiments by Yanuar *et al.,* [14, 15]. Limitations hydrodynamic references of the warp-chine hull in the multihull, although some of the studies mentioned earlier have shown their superiority compared to another hull form. Therefore, this research about the hydrodynamic warp-chine on the pentamaran focuses on wave resistance and total resistance at a speed range corresponding to high wave resistance. The model was assembled as an arrow as trimaran formation in various configurations suggested from the optimum hull of multihulls. A series of tests were carried out on lateral separation or clearance of the front-side hull as CL_1 on 1.05 Bmh and 1.2 Bmh, clearance of the after-side hull as CL_2 on 1.2 Bmh and 1.5 Bmh, and longitudinal distance or stagger as S_T on 0.35L, 0.42L and 0.5L. The analysis was done using a computational solver based on Michell's integral, fixed by Tuck and Lazauskas [16] and validated by a test model on a towing test.

2. Methodology

2.1. Wave Resistance Based on Michell's Theory

The expression provided by Michell [17] for the wave resistance based on beam/length ratio was thin ship. According to Tuck and Lazauskas [16], Michell's investigation of the wave produced by a ship could be rapid, accurate and also capable of fine detail of wave pattern.

2.2. Multihull Resistance

In this study, a pentamaran was used with the main hull representing as a hard chine recommended by Savitsky and four identical V forms as outriggers. The two side hulls (outriggers) located on the portside and starboard as a trimaran formation were presented in Figure 1. And the pentamaran dimension were described in Table 1. Related to the warp-chine hull form that can reduce the drag of pentamaran accuracy of stagger, clearance and Froude number (Fn). This study sets the distance of the center of first clearance (CL_1) of the front-side hull to the center of the main hull are 1.05 and 1.2 of the main hull beam (Bmh). The second clearance (CL_2) of the center of the

after-side hull to the center of the main hull beam (Bmh) are 1.2 and 1.5 of the main hull beam (Bmh). For stagger (S_T), which is the distance from the transom of the side hull to the transom of the main hull is 0.36, 0.42 and 0.5 of the mainhull waterline length (L_{WL}).

Some of the researchers, i.e. Tuck and Lazauskas [9], Moraes [10], Hanhirova [18], Peng [19], Day *et al.,* [20] and Yeung *et al.,* [21], agreed that wave resistance of a high-speed monohull and multihull as given by Michell's integral was quite good with computed values in a towing test. The characteristic of the hull shape allows interference factors between the divergent and the transverse systems to generate wave resistance. By increasing the ship speed, the energy produced from the movement of the ship will be absorbed more by the transverse than the divergent system, leading to a strong behaviour interference. Hence, it took a good choice in determining the exact hull placement in a pentamaran in order to cancel the wave and minimise interference.

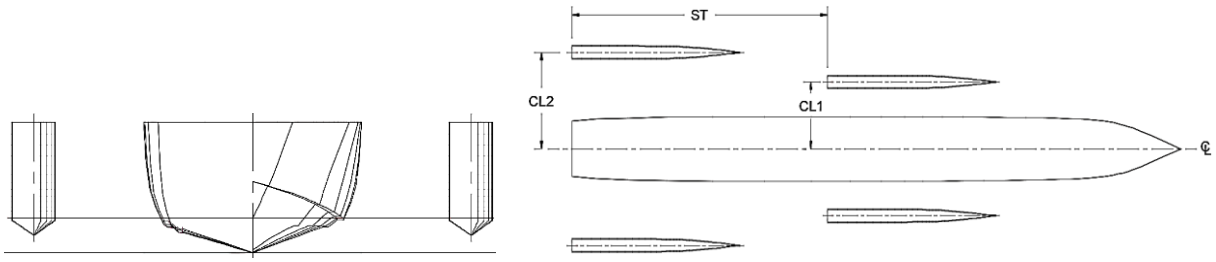

Fig. 1. Hull plan model and set-up pentamaran configuration

Table 1
Main dimension of model pentamaran

Dimension	Main hull	Outrigger
WL length (mm)	1435.9	414
Beam on WL (mm)	126.7	30
Draft (mm)	24	12
Height (mm)	90	78
Deadrise (degree)	20	35
Wetted area (mm^2)	17.68×10^4	14.87×10^3
Volume(displacement) (mm^3)	20.45×10^5	69.01×10^3
Displacement (Kg)	2.0378	0.0688
Total Displacement (Kg)	2.313	

The wave resistance based on Michell's, the stream energy far from the ship explain the wave heights of inducing the actual wave resistance (Rw) by free-wave spectrum integration to the angle of propagation (θ).

$$R_W = \frac{\pi}{2}\rho U^2 \int_{-\frac{\pi}{2}}^{\frac{\pi}{2}} |A(\theta)|^2 cos^3\theta \, d\theta \quad (1)$$

The flow quantities of wave resistance represent wave elevation z = Z(x, y), which is created by hull Y(x, y).

$$A(\theta) = -\frac{2i}{\pi} k_0^2 \, sec^4\theta \iint Y(x,y) \, exp(k_0 z \, sec^2\theta + ik_0 x \, sec\theta) \, dxdz \quad (2)$$

Hull was integrated with transom stern require modification of Eq. (2) which indicated by Y (xs, z) as offset transom:

$$A(\theta) = -{}^{2i}/_{\pi}\,(k_0 sec^2\theta)^2 \int_{-\infty}^{0}\int_{-\infty}^{\infty} Y(x,z)e^{ik_0 x sec\theta}\, e^{k_0 z sec^2\theta} dxdz + {}^{2}/_{\pi}\,(k_0 sec^3\theta)\int_{-\infty}^{0} Y(x_s,z)\, e^{k_0 z sec^2\theta} dxdz \quad (3)$$

k (θ) = $k_0 \sec^2\theta$; $k_0 = g/U^2$, g is gravity, and U is ship speed. Where wave pattern of ship, ς(x,y)

$$\varsigma(x,y) = R_W \int_{-\frac{\pi}{2}}^{\frac{\pi}{2}} A(\theta) e^{-ik(\theta)[x\cos\theta + y\sin\theta]} d\theta \quad (4)$$

is generated from wave propagation at various angles θ to the x-axis direction of the ship's motion. A nondimensional wave resistance coefficient (Cw) presented as

$$C_W = {}^{R_W}/_{1/2\,\rho U^2 S} \quad (5)$$

where ρ for water density, U forward speed, and S ship wetted area. Then, for the viscous resistance was using the International Towing Tank Conference (ITTC) 1957 line to determined coefficient friction (C_F)

$$C_F = {}^{0.075}/_{(log_{10}Rn - 2)^2} \quad (6)$$

and Prohaska method is used in the form factor (k + 1) by utilizing test data at low Froude numbers (0.12 < Fr < 0.24).

$$C_V = (1+k)C_F \quad (7)$$

For multihull with N hulls, j numbered of hull is located at $(x,y) = (x_j,y_j)$, $A_j(\theta)$ wave amplitude, then the total far-field wave is

$$\varsigma(x,y) = \sum_{j=1}^{N} R_W \int_{-\frac{\pi}{2}}^{\frac{\pi}{2}} A_j(\theta) e^{-ik(\theta)[(x-\mathrm{xj})\cos\theta + (y-yj)\sin\theta]} d\theta \quad (8)$$

$$\varsigma(x,y) = R_W \int_{-\frac{\pi}{2}}^{\frac{\pi}{2}} e^{-ik(\theta)[x\cos\theta + y\sin\theta]} \sum_{j=1}^{N} A_j\, e^{ik(\theta)[x_j\cos\theta + y_j\sin\theta]} d\theta \quad (9)$$

where amplitude function in Eq. (8) is modified from the expression Eq. (2) to

$$A(\theta) = \sum_{j=1}^{N} A_j(\theta) e^{ik(\theta)[xj\cos\theta + yj\sin\theta]} \quad (10)$$

$$A_j(\theta) = \sigma_j A_0(\theta) \quad (11)$$

σ_j represents the fraction of the total displacement of multihull. Then the following expression is given for combined wave amplitude A(θ)

$$A(\theta) = A_0(\theta)\, F(\theta) \quad (12)$$

F(θ) as interference between the hulls is

$$F(\theta) = \int_{j=1}^{N} \sigma j e^{ik(\theta)[xj\ cos\theta + yj\ sin\theta]} \quad (13)$$

where F(θ) is an independent factor of wave-making of individual hulls measured by $A_0(\theta)$.

2.3. Interference Resistance

Generation of low resistance on multihull with warp-chine can be performed by evaluating the design of hull forms on varying parameters such as deadrise angle. In addition, the interaction between hulls that can build wave interference and whisker spray interference should also be taken into consideration. Several studies about the optimum of warp-chine, i.e. Begovic and Bertorello [12], Bari and Matveev [13], Savitsky [22], Ghassemi [23], Taunton *et al.,* [24] and Schachter [25], focused on the deadrise angle 20° for the main hull and 35° for the side hulls.

Tuck and Lazauskas [9] provided an assumption that transverse waves can eliminate with determined main hull on a half of total displacement and each side hulls on a quarter (σ = 1/4), which staggered longitudinally by an odd multiple of a half wavelength and that stagger s = π/k_0 takes the minimum value to cancel transverse waves. The total resistance minimisation of multihull determined by individual outrigger displacement (σ), stagger (s), clearance (w) on minimising complex expression Eq. (13) with G (θ) is

$$G(\theta) = |F(\theta)|^2 \quad (14)$$

References on multihull interferences were also given by Gotman [26], and even Tuck [16, 27] used Michell's thin-ship theory to develop a computational program 'Michlet' [28] for resistance components and wave spectrum, which appear from the effect of hull shape and hull placement. This tool was by input set of offsets (red dot) defining the hull ship y = ±Y(x, y) for wave elevation z = Z(x, y) points or free-wave spectrum, which are presented in a grid data as shown in Figure 2(a), described as a body with waterlines and section. Figure 2(b) shows the coordinate system of pentamaran measured relatively to the main hull (as the origin) indicating a nominal point x = s_i, y = w and z = 0.

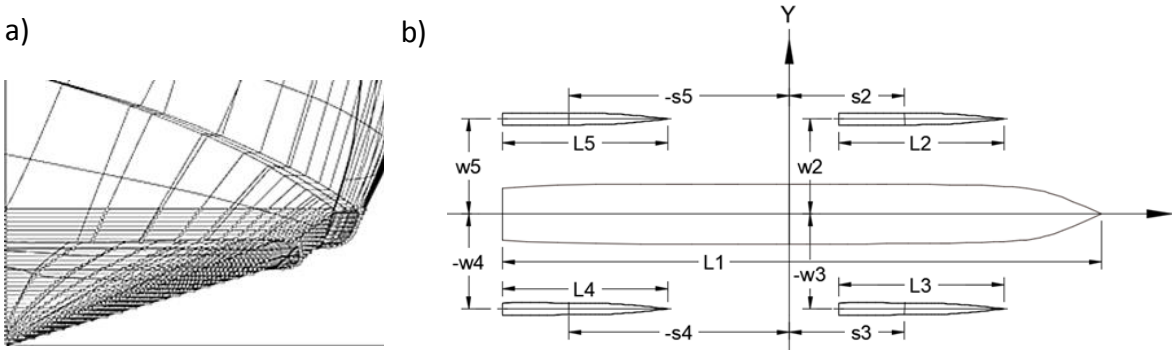

Fig. 2. (a) Offsets defining the main hull; (b) coordinates system program of pentamaran

2.4. Towing Test Set-Up

The tests on the calm water were conducted in the towing tank of Institut Teknologi Sepuluh Nopember (ITS) Surabaya. Its principal dimensions are 50 m, 3 m and 2 m for the length, width and depth, respectively. The tank is equipped with three cameras mounted on the front of the right side, the centre between the main hull and the side hull, as well as on the centre of the stern. The

set-up test of the model to be even keel at the design drafts and the geometrical design is summarized in Table 1, in which the models were made from fibreglass coated with epoxy to smoothly attach on the surfaces of the hull. The test range of Froude number, Fn = U/(g.L)0.5, is from 0.1 to 0.6, corresponding to model speeds between 0.58 m/s and 2.30 m/s. In Figure 1, there are six variations of towing-tank test hull configurations, and detailed test schemes and hull spacings were described in Table 2.

Table 2
Model test configurations

Configuration	Stagger (m)	Cl-1 (m)	Cl-2 (m)
A	0.36L	1.20Bmh	1.20Bmh
B	0.36L	1.05Bmh	1.50Bmh
C	0.42L	1.20Bmh	1.20Bmh
D	0.42L	1.05Bmh	1.50Bmh
E	0.50L	1.20Bmh	1.20Bmh
F	0.50L	1.05Bmh	1.50Bmh

3. Result

3.1. Comparison of All Configurations

3.1.1. Computation results

The report computations as shown from Figure 3 to Figure 5 were using Michell's integral for coefficient of: wave, interference and total resistance.

Figure 3 shows the results of all configurations for the transversal wave coefficient in (a) Cw-trans and the divergent wave coefficient in (b) Cw-div. It can be seen that Cw-trans tends to rise to the highest transversal wave at Fn above 0.5, and then its value gradually falls. While Cw-div, the highest value starts at Fn 0.4 and it gradually decreases. The highest Cw-trans is obtained successively by models A and B, then C and D and the lowest E and F, while the highest Cw-div is obtained by F and A, then C and E and the lowest B.

Figure 4 (a) presents graphs of wave coefficient, Cw, which have similarity trend with the divergent wave in Figure 3(b). At range Fn 0.5–0.6, model F still has the lowest Cw from all configurations, demonstrating that the divergent waves predominate at high speeds. For the interference wave coefficient, Cw-int, model F has the lowest interference (negative interference) at low Fn < 0.5, but model A has the highest, precisely at Fn 0.45, as shown in Figure 4(b). The negative interference represents less wave resistance of cross waves between hulls. It can be seen that parallel to the increasing Fn, all trends of configurations almost coincide with model C, which has the lowest interference at high Fn (1.0).

For the total resistance, CT, results are given in Figure 5. It can be seen that all configurations have an increasing trend at Fn 0.4, and then decreases, same as in Figure 3 (b) and Figure 4 (a).

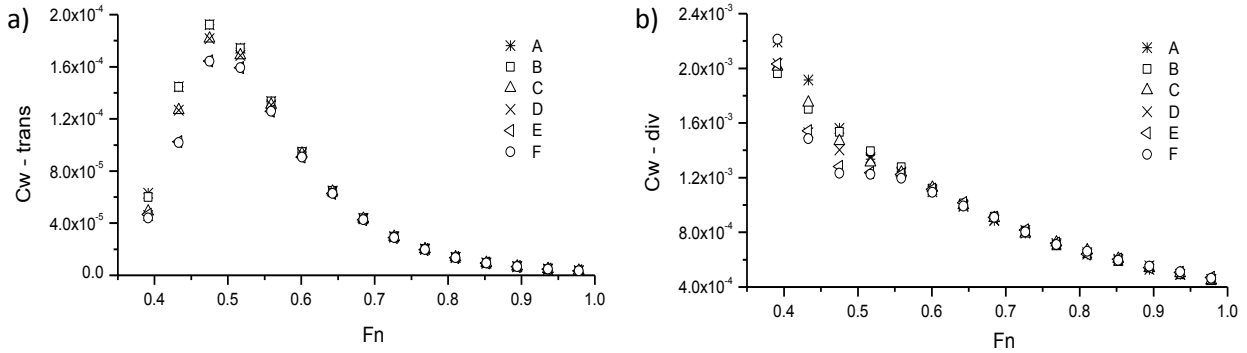

Fig. 3. Results of computational calculation based on 'Michell': (a) coefficient of transverse wave, Cw-trans; (b) coefficient of divergent wave, Cw-div

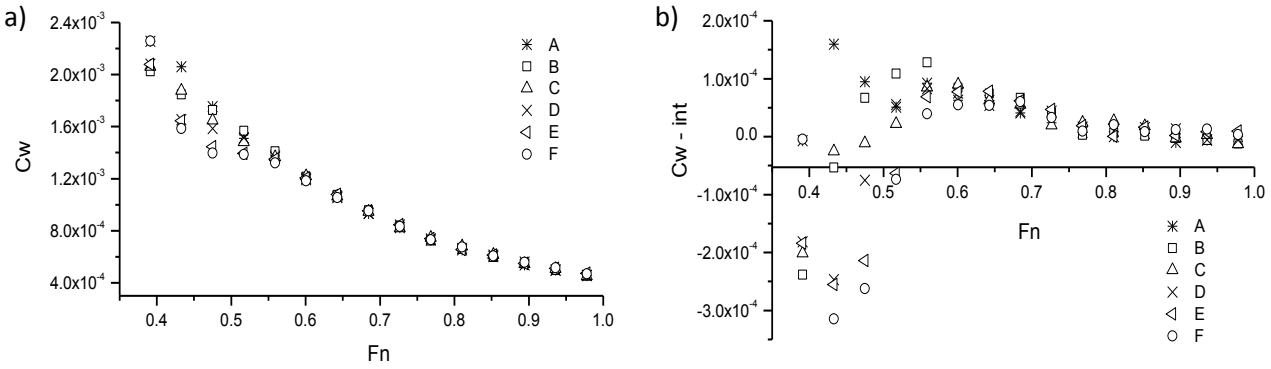

Fig. 4. Results of computational based on 'Michell': (a) coefficient of wave resistance, Cw; (b) interference resistance, Cw-int

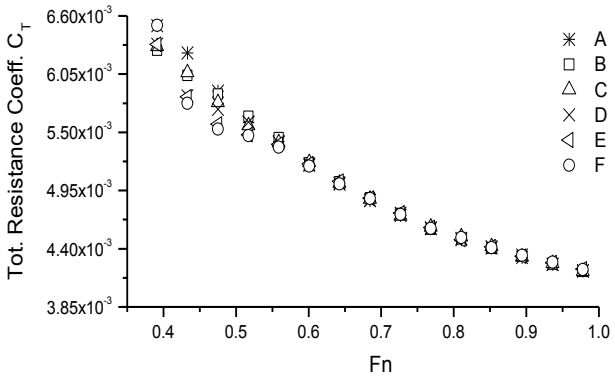

Fig. 5. Results of computational based on 'Michell'on total resistance, C_T

3.2. Comparison between Test and Computational

The comparison between computational calculation and test of wave resistance and total resistance is presented in Figures 6 to 8. For the test calculation, 'Prohaska' method was used to determine the form factor and the International Towing Tank Conference (ITTC) 1957 line for friction coefficient Eq. (6).

The results show that at stagger of 0.36L, 0.42L and 0.5L, the trends of all configurations were consistent with the test at Fn > 0.5. In the test model at stagger of 0.36L, the average of the wave and the total resistance of models A and B decreases by 15.13% and 0.879%, while in the computational calculation, the average of the wave and the total resistance increase by 1.739% and 0.375%, respectively. At stagger of 0.42L, as shown in Figure 6, the trend of the wave resistance

coefficient of models C and D is similar with that in Figure 7. The average wave resistance in the test model decreases by 19.766%, but the total resistance increases by 7.793%, while in the computational calculation, both the wave and the total resistance decrease by 1.193% and 0.188%, respectively. For models E and F in Figure 8, there is a slightly different trend compared to others i.e. the average wave resistance decreases by 21.663% and the total resistance increases by 1.6%. In the computational calculation, both the wave and the total resistance decrease by 2.037% and 0.443%, respectively.

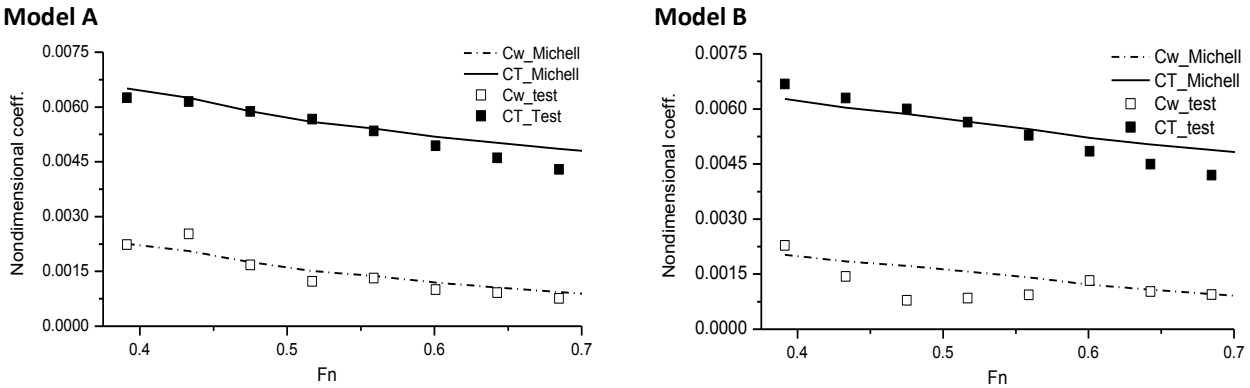

Fig. 6. Comparison between test and computational on stagger 0.36L

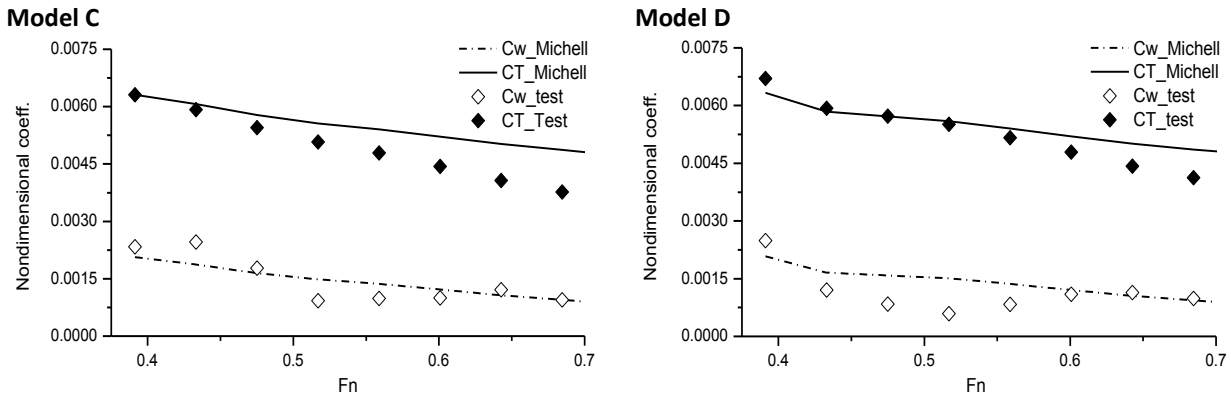

Fig. 7. Comparison between test and computational on stagger 0.42L

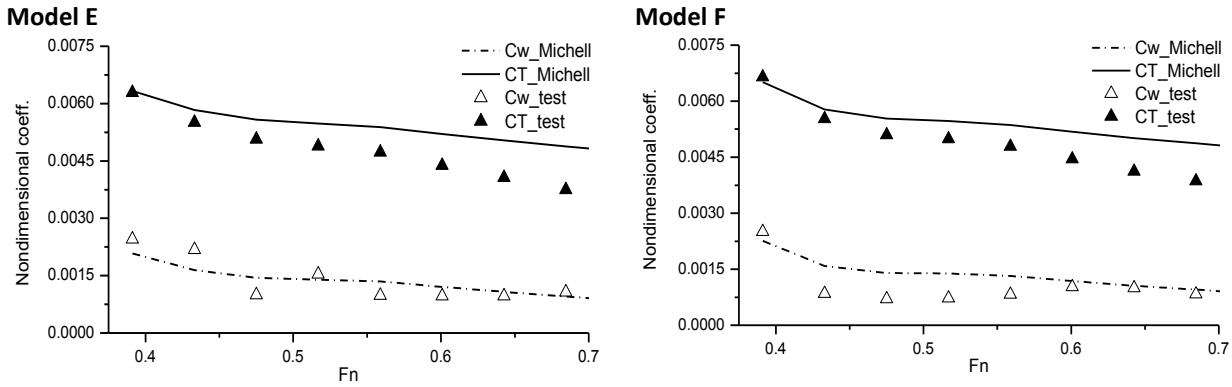

Fig. 8. Comparison between test and computational on stagger 0.5L

Changing at stagger 1.2 Bmh where CL1–CL2 is in the same line with models A, C, and E, the model test results show that both the wave and the total resistance are decreasing on average: A to C, 0.985% and 10.188%; C to E, 4.521% and 2.609%. In the computational calculation, both the

wave and the total resistance have decreased: A to C, 1.090% and 0.344%; C to E, 3.798% and 0.879%, respectively. And changing at stagger where CL1–CL2 is not in the same line with models B, D and F, in general, gives decreasing results of the test model on both the wave and the total resistance: B to D, 6.386% and 2.332%; D to F, 6.778% and 8.204%. Moreover, the results of the computational calculation also show a reduction on both the wave and the total resistance: B to D by 3.942% and 0.903%; D to F by 4.619% and 1.132%.

3.3. Far-Field Wave Pattern

The wave spectra were illustrated in Figure 9 and Figure 10 at Fn 0.6 on provides 'Michlet' program, which is a linear superposition of the far-field free-wave patterns on the sectoral patch, an area of the back of the ship. The colour indicates the value of Z (x, y), with dark blue indicating the deepest troughs and nearly white indicating the highest crests.

Figure 9 shows a similar wave pattern of models A, C, and E that had produced deeper and wider divergent waves illustrated by sharp contours of blue and wide. Whereas the enveloping wedge of models B, D, and F has widened slightly with lighter blue as shown in Figure 10.

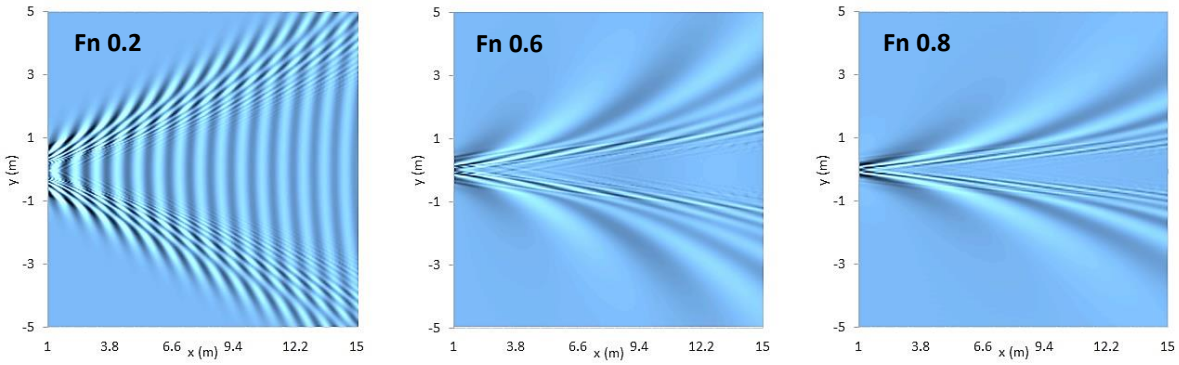

Fig. 9. Characteristics of far-field wave pattern of models A, C and E at Fn 0.6

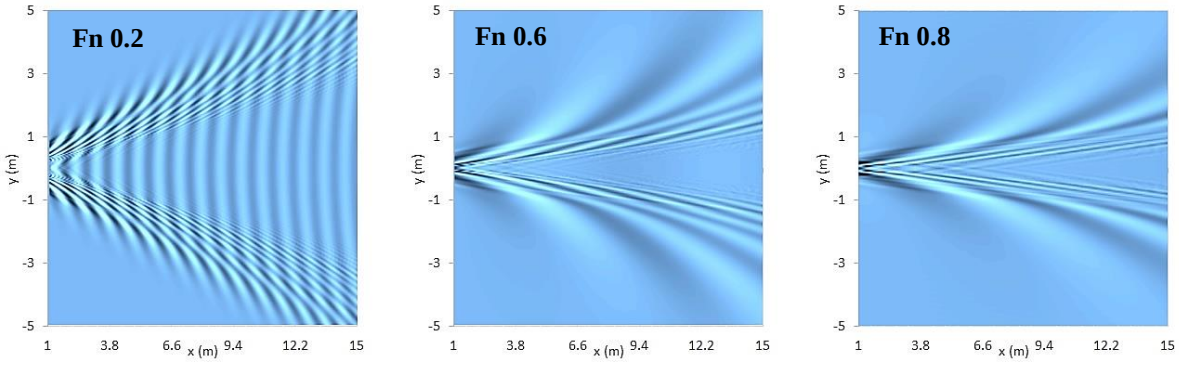

Fig. 10. Characteristics of far-field wave pattern of B, D and F at Fn 0.6

3.4. Discussion

The comparative analysis of the computational reports and the measurement test on waves and total resistance had quite a similar trend above Fn 0.5. The average deviations of the total resistance coefficient (C_T) were obtained: 1.78% for A, 0.67% for B, 6.85% for C, 0.73% for D, 8.70% for E, and 6.89% for F. The average deviations of the wave resistance coefficient (Cw) were: 2.78% for A, 20.55% for B, 0.44% for C, 21.53% for D, 1.26% for E, and 25.17% for F. This comparative analysis proves that the computation "Michlet" tool adequate in respect of the total resistance

measurement accuracy but poor agreement for wave resistance. We previously had predicted this likely deviation owing to difficulties in determining the correct form factor (1+k) of the multihull (7).

All configurations report has an increasing trend below Fn 0.5 and then decrease afterward. We suppose the complexity of the interference factor at high speeds generate the destructive wave of hull-to-hull interaction and dominant in influencing the magnitude results of the wave resistance. It is related to the configuration of the multihull. And finally, directly affects the reduction in total resistance.

The angle of the line between the centreline of the main hull to each of centreline of the front-side hull of models B, D and F approximately 15°-18° has a good cancellation to transverse wave that is appropriate with Tuck and Lazaukas [9] for the ship with arrow tri-hull.

Referring to the wave pattern of the computational program 'Michlet' at Fn > 0.5 from Figures 9 and 10 indicates conformity with the test as shown in Figures 11 and 12 (left figure). The model where CL1–CL2 is in the same line (A, C and E) had some degree of reduction within a certain range of Fn, likewise at the model where CL1–CL2 is not in the same line (B, D, and F). But generally, the clearance at CL1–CL2 is not in the same line give more reduction on the wave and total resistance. The boundary layer and wake due to the shape of the hull, as well as the placement of the side hull in such a way that it reduces the interference of the bow and the stern wave systems.

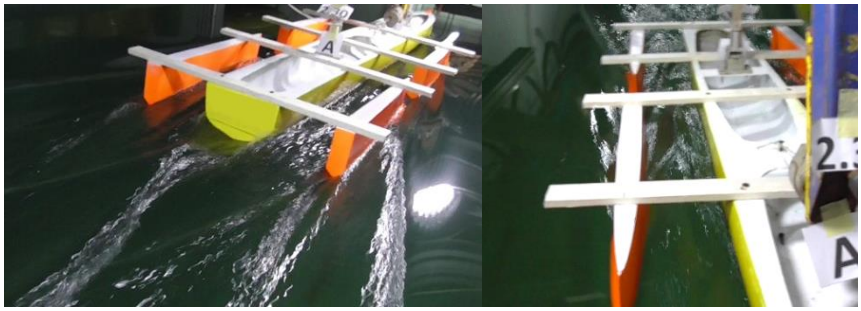

Fig. 11. Wave characteristic of test results of models A, C and E at Fn 0.6 between the main hull and the side hull (right), and after stern (left)

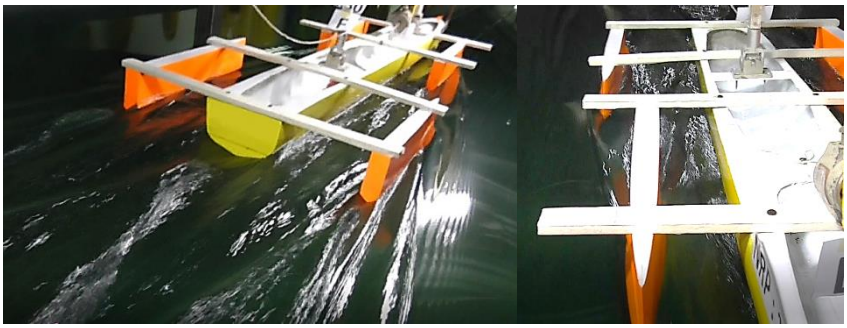

Fig. 12. Wave characteristic of test results of models B, D and F at Fn 0.6 between the main hull and the side hull (right), and after stern (left)

4. Conclusion

The tests have been performed in compliance with the ITTC standards. It is agreed that the computational reports and the measurement test on waves and total resistance had indeed a similar trend, although there were some discrepancies at range Fn 0.4–0.5. More length at stagger would increase the total resistance due to unfavourable wave interference between hulls. But changing of the side hull on clearance strongly affects the resistance characteristics than that on stagger as shown on models B, D and F, where the trend resistance interference of all models

tends to decrease when increasing hull separation with the front-side hull closer to the main hull. Aligning placement of the main hull to the side hull with formation arrow tri-hull near to Kelvin angle would cancel the wave formed by the leading hull. In general, thin-ship theory by Michell which predicts the coefficient component resistance of model with warped chine yields quite good results in the towing test.

Further work must be undertaken with regard to optimization of clearance and stagger to verify the best minimum resistance. Less resistance means reduced use of horsepower (power energy), hence resulting in reduced fuel consumption.

Acknowledgement

The first author acknowledges the support by the Indonesian Endowment Fund for Education (LPDP). We would like to thank the technicians and laboratory staff of the Institut Teknologi Sepuluh Nopember (ITS)'s towing tank in this research.

References

[1] Ikeda, Yoshiho, Emiko Nakabayashi, and Ai Ito. "Concept design of a pentamaran type fast RoRo ship". *Journal of the Japan Society of Naval Architects and Ocean Engineers*, 1 (2005): 35-42.
[2] Oller, Erik, Vasilios Nikou, & Konstantinos Psallidas. Focused Mission High Speed Combatant. DTIC Document, 2003.
[3] Daniel Savitsky. "Some interference effects between two flat surfaces planing parallel to each other at high speed." *Journal of the Aeronautical Sciences* 21, no. 6 (1954): 419-420.
[4] Ocon, Joey Duran, Ludek Jirkovsky, Rizalinda L. de Leon, and Amador Muriel. "Theory-derived law of the wall for parallel flat-plates turbulent flow." *CFD Letters* 4, no. 3 (2012): 93-101.
[5] Liu, C.Y., Wang, C.T. "Interference effects of catamaran planing hulls." *Journal of Hydronautics* 13. no. 1 (1979): 31-32.
[6] Savitsky, Daniel. "Hydrodynamic design of planing hulls." *Marine technology* 1, no. 1 (1964).
[7] Chengyi, Wang. Resistance charicteristic of high-speed catamaran and its application. Shipbuilding of China 3:003, 1994.
[8] BENJAMIN, B. ACKERS. "An investigation of the resistance characteristics of powered trimaran side-hull configurations." *Transaction of SNAME* 105 (1997): 349-373.
[9] Tuck, Ernest O, & Leo Lazauskas. "Optimum hull spacing of a family of multihulls." *Ship Technology Research-Schiffstechnik* 45, no.4 (1998): 180.
[10] Moraes, H. B., J. M. Vasconcellos, and R. G. Latorre. "Wave resistance for high-speed catamarans." *Ocean Engineering* 31, no. 17-18 (2004): 2253-2282.
[11] Blount, DL, & JA McGrath. "Resistance characteristics of semi-displacement mega yacht hull forms." *Trans. RINA, Intl. J. Small Craft Tech* 151 (2009).
[12] Begovic, E, & C Bertorello. "Resistance assessment of warped hullform." *Ocean Engineering* 56, (2012): 28-42.
[13] Bari, Ghazi S, & Konstantin I Matveev. "Hydrodynamic modeling of planing catamarans with symmetric hulls." *Ocean Engineering* 115 (2016): 60-66.
[14] Yanuar, Gunawan, Kurniawan T. Waskito, and A. Jamaluddin. "Experimental Study Resistances of Asymmetrical Pentamaran Model with Separation and Staggered Hull Variation of Inner Side-hulls." *International Journal of Fluid Mechanics Research,* (2015): 82-94.
[15] Yanuar, Ibadurrahman, M.H Faiz and M.H. Adib. "Experimental Analysis of Diamond Pentamaran Model with Symmetric and Asymmetric Hull Combinations." *Journal of Engineering and Applied Sciences* 12, no.13 (2017): 3434-3440.
[16] Tuck, E. O., D. C. Scullen, and L. Lazauskas. "Wave patterns and minimum wave resistance for high-speed vessels." *In 24th Symposium on Naval Hydrodynamics, Fukuoka, Japan*, vol. 813. 2002.
[17] Michell, John Henry. "XI. The wave-resistance of a ship." *The London, Edinburgh, and Dublin Philosophical Magazine and Journal of Science* 45, no. 272 (1898): 106-123.
[18] Hanhirova, K., S. Rintala, and T. Karppinen. "Preliminary resistance prediction method for fast mono-and multihull vessels." (1995).
[19] Peng, Hongxuan. "Numerical computation of multi-hull ship resistance and motion." (2001).
[20] Clelland, D., A. H. Day, and E. Nixon. "Experimental and numerical investigation of'Arrow'trimarans." In *7th International Conference of Fast Sea Transportation.* 2003.

[21] Yeung, Ronald W., Gregoire Poupard, Jean O. Toilliez, Heinrich SÖDING, A. Sh GOTMAN, and Hendrik F. VAN HEMMEN. "Interference-resistance prediction and its applications to optimal multi-hull configuration design. Discussion." *Transactions-Society of Naval Architects and Marine Engineers* 112 (2004): 142-168.
[22] Savitsky, Daniel, Michael F. DeLorme, and Raju Datla. "Inclusion of whisker spray drag in performance prediction method for high-speed planing hulls." *Marine Technology* 44, no. 1 (2007): 35-56.
[23] Hassan Ghassemi & Mahmoud Ghiasi. "A combined method for the hydrodynamic characteristics of planing crafts." *Ocean Engineering* 35, (2008): 310–322.
[24] Taunton, D. J., D. A. Hudson, and R. A. Shenoi. "Characteristics of a series of high speed hard chine planing hulls-part II: performance in waves." *International Journal of Small Craft Technology* 153 (2011): B1-B22.
[25] Schachter, R. D., H. J. C. Ribeiro, and C. A. L. da Conceição. "Dynamic equilibrium evaluation for planing hulls with arbitrary geometry and variable deadrise angles–The virtual prismatic hulls method." *Ocean Engineering* 115 (2016): 67-92.
[26] Gotman, A. Sh. "Study of Michell's integral and influence of viscosity and ship hull form on wave resistance." *Oceanic Engineering International* 6, no.2 (2002): 74–115.
[27] Tuck, E. O., D. C. Scullen, and L. Lazauskas. "Sea wave pattern evaluation, part 4 report: extension to multihulls and finite depth." *In Department, The University of Adelaide*. 2000.
[28] Algie, Cam, Tim Gourlay, Leo Lazauskas, and Hoyte Raven. "Application of potential flow methods to fast displacement ships at transcritical speeds in shallow water." *Applied Ocean Research* 71 (2018): 11-19.